Available online at www.sciencedirect.com

SciVerse ScienceDirect

Ceramics International 38 (2012) 5023–5026

CERAMICS INTERNATIONAL

www.elsevier.com/locate/ceramint

Synthesis and thermoelectric performance of Li-doped NiO ceramics

Shaohui Liu [a], Jiao Wang [a], Jianfeng Jia [a,*], Xing Hu [a], Shijiang Liu [b]

[a] School of Physical Engineering and Laboratory of Material Physics, Zhengzhou University, Zhengzhou 450052, PR China
[b] College of Physics and Electric Information, Luoyang Normal University, Luoyang 471022, PR China

Received 13 February 2012; received in revised form 29 February 2012; accepted 29 February 2012
Available online 7 March 2012

Abstract

$Ni_{1-x}Li_xO$ ($x = 0$, 0.03, 0.06, 0.09) powders were prepared by sol–gel method combined with sintering procedure using $Ni(CH_3COO)_2{\cdot}4H_2O$ and citric acid as the raw materials and alcohol as solvent. The crystal structures of the samples were investigated by X-ray diffraction and Raman spectroscopy. The thermoelectric properties, such as the electrical conductivity, the Seebeck coefficient and the thermal conductivity were measured. The results showed that all the samples are p-type semiconductors. The electrical conductivity increases with the increase of the temperature, which indicates that the substitution of Li^+ for Ni^{2+} can increase the concentrations and mobility of the carriers. The thermal conductivity decreases remarkably with the increase of the Li doping content, which indicates that Li doping can enhance the scattering of phonon. However, the Seebeck coefficient will decline with the increase of the Li doping content. As results of the increase of electrical conductivity and reduction of thermal conductivity, Li doping can increase the figure of merit (*ZT*) of NiO, the *ZT* value reach 0.049 at 770 K for $Ni_{1-x}Li_xO$ with $x = 0.06$.

Keywords: Thermoelectric properties; NiO; Li doping

1. Introduction

Thermoelectric (TE) materials are currently gaining worldwide interest because of their great potential applications in fields such as converting waste heat into electricity or refrigerating without any moving element [1]. The quality of a thermoelectric material can be evaluated by its dimensionless figure of merit *ZT* and $ZT = \alpha^2\sigma T/\kappa$ (where α, σ, κ and T are Seebeck coefficient, electrical conductivity, thermal conductivity, and absolute temperature, respectively). The figure of merit indicated that a qualified thermoelectric material should have a high Seebeck coefficient, a high electrical conductivity, meanwhile a low thermal conductivity. However, due to the correlations between α, σ, and κ, it is very difficult to optimize them synchronously [2–4]. Up to date, the doped alloy TE materials based on Bi_2Te_3 are the best known ones with $ZT \approx 1$ at room temperature [5]. However, because of easy being oxidized and vaporization, the alloy TE materials cannot be used for applications at high-temperature in air. Therefore, the oxide TE materials, such as $Ca_3Co_4O_9$ and other oxides that can be used at high-temperature and in oxygen, also cause widely attentions in recent years [6].

NiO is a 3d transition metal oxide with a simple cubic structure which has been reported to be a potential candidate thermoelectric material for applications at high-temperature in air [7]. Earlier studies have showed that its electric conductivity will increase when doped by Li, and further research on highly Li-doped NiO showed that its TE property at high temperature can be comparable to other oxide TE materials. Powders of NiO had been prepared by coprecipitation method [8], sol–gel techniques [9], and hydrothermal route [10]. Compared with other methods, sol–gel method is a simple, versatile and convenient approach to manufacture materials. It is believed that the large thermoelectric power of $Ca_3Co_4O_9$ is caused by strong electron–electron correlation due to its narrow 3d metal band [11], the electrical transport properties of the 3d transition metal oxide $Ni_{1-x}Li_xO$ should have some similarity with the $Ca_3Co_4O_9$. However, there were few reports on $Ni_{1-x}Li_xO$ as new oxide thermoelectric material, and it is necessary to perform systematic investigation to gain insight into the effects of Li doping on thermoelectric properties of NiO. In this paper, we use sol–gel method combined with sintering procedure to

* Corresponding author.
E-mail address: Jiajf@zzu.edu.cn (J. Jia).

0272-8842/$36.00
doi:10.1016/j.ceramint.2012.02.099

make $Ni_{1-x}Li_xO$ ($x = 0$, 0.03, 0.06, 0.09) samples and investigate the effect of Li doping on their thermoelectric properties.

2. Experimental

The precursor of $Ni_{1-x}Li_xO$ powders was prepared as follows: 1 g citric acid was dissolved into 25 ml alcohol with stirring at room temperature. Then 2 g $Ni(CH_3COO)_2{\cdot}4H_2O$ and the suitable amount of $CH_3COOLi{\cdot}H_2O$ with different atomic ratios (Ni:Li = 100:0, 100:3, 100:6 and 100:9) were added slowly into the solution under vigorous stirring at 40 °C for 2 h. Ultimately, a lucid and viscous sol solution was obtained and the sol solution was heated at 80 °C until a green viscous wet gel was obtained. Then the wet gel was dried in a desiccator at 90 °C for 8 h, and a green fluffy dry gel was obtained. After calcining at 700 °C for 3 h in air, pure NiO and Li-doped NiO powders were obtained.

X-ray diffraction (XRD) was employed to investigate the crystal structure of powders using Cu/Kα radiation. Besides, Raman scattering spectroscopy with the Ar^+ (514.5 nm) laser lines as the excitation source was used to examine the vibration modes of the crystal lattice to identify the compositions in the powders.

To investigate the thermoelectric properties of NiO-based oxide, the $Ni_{1-x}Li_xO$ powders were pressed into pellets and then the pellets were calcined in furnace at 1200 °C for 6 h. The pellets were cut into 1.4 mm × 5 mm × 15 mm rectangular bar for the conductivity and Seebeck coefficient measurement. Electrical conductivity and Seebeck coefficient were measured at several temperature points using a four-probe technique on a custom designed apparatus. The thermal conductivities of the pellets were measured by a thermal diffusion system (FLASHLINE™ 3000, ANTER) using Pyroceram (Provided by ANTER) as reference sample at several temperature points.

3. Results and discussion

Fig. 1 shows the XRD patterns of the $Ni_{1-x}Li_xO$ samples. It can be seen that five Bragg reflections at $2\theta = 37.2°$, 43.4°, 62.9°, 75.2° and 79.4° corresponding to (1 1 1), (2 0 0), (2 2 0), (3 1 1) and (2 2 2) characteristic peaks of the cubic crystalline NiO. This indicates that there are no impurity phases exists in the Li doped samples with the sensitivity of XRD measurement. The inset of Fig. 1 shows the expanded XRD patterns corresponding to the (2 0 0) characteristic peak, which clearly indicates that the diffraction peak shifts to high angle when Li doping amount become high. The lattice constant of the Li-doped samples is shown in Fig. 2, which indicates that the lattice constant will reduce with the increase of the Li concentration. This is because that the radius of Li^+ ion is 5% smaller than that of Ni^{2+}, the substitution of Li^+ for Ni^{2+} will cause a reduction of the lattice constant.

Fig. 3 shows the room temperature Raman spectrum of the $Ni_{1-x}Li_xO$ powders. Two Raman peaks located at about 570 and 1100 cm^{-1} are observed. The former is corresponding to the one-phonon (1P) transverse optical (TO) and longitudinal optical (LO) phonon modes of NiO. The latter can be assigned to two-phonon (2P) 2LO modes. Whether having Li dope or not, the positions of Raman peaks have no obvious shift. Combining with the results of XRD spectra discussed above, it indicates that small amounts of Li doping will not change the crystal structure. However, it should be noted that with the increase of Li^+ concentration, the full widths at half maximum (FWHM) of the Raman peaks become broad and their height decrease, and the first-order Raman scattering peak at 1100 cm^{-1} almost disappears for the Li doped samples. This indicates that the stochastic distribution of Li^+ as heterogeneous ion in the NiO crystal lattice enhances the scattering of phonons, which could induce the decrease of thermal conductivity.

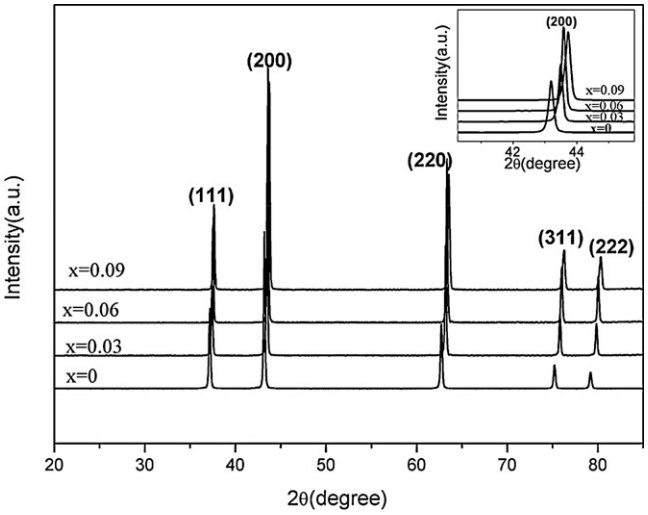

Fig. 1. XRD patterns of $Ni_{1-x}Li_xO$ ($x = 0$, 0.03, 0.06, 0.09).

The temperature dependence of the thermal conductivity (κ) is plotted in Fig. 4, from which we can find that the value of κ decreases with the increase of Li concentration, which is accordant with the conclusions from the Raman spectra. Moreover, the value of κ decreases with the increase of temperature. The total κ can be written as $\kappa = \kappa_{ph} + \kappa_e$, where κ_{ph} and κ_e are thermal conductivity due to phonon and electron,

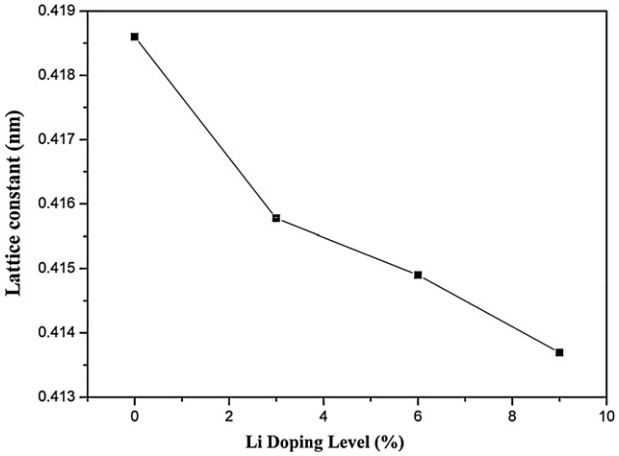

Fig. 2. Lattice constants of $Ni_{1-x}Li_xO$ ($x = 0$, 0.03, 0.06, 0.09).

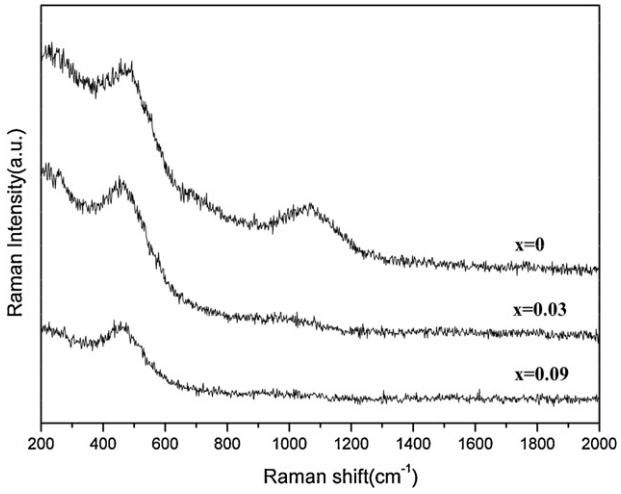

Fig. 3. The room temperature Raman spectrum of $Ni_{1-x}Li_xO$ powders.

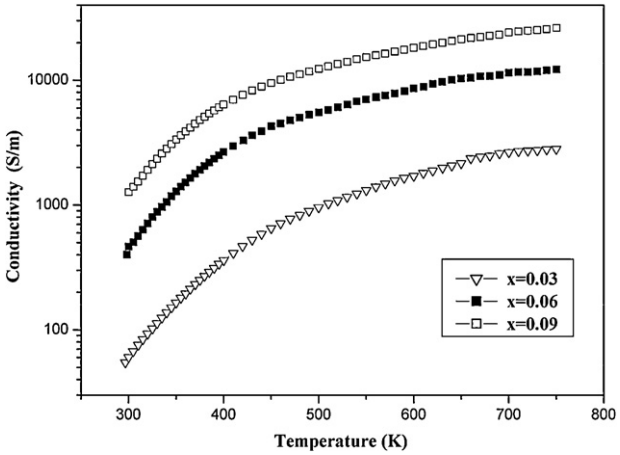

Fig. 5. Temperature dependence of electrical conductivity for $Ni_{1-x}Li_xO$.

Table 1
Activation energy (E_a) of $Ni_{1-x}Li_xO$.

Li (mol%)	Slope	E_a (eV)
0	–	0.528
3	1964	0.169
6	1626	0.140
9	1455	0.125

respectively. Usually, comparing to κ_{ph}, κ_e of a semiconductor is very small according to the Wiedmann–Franz Law $\kappa_e = LT\sigma$, where L is the Lorentz number (1.5×10^{-8} W Ω K^{-1}). The contribution of electrons to total κ is much small than that of phonon at the measured temperature range, so $\kappa \approx \kappa_{ph}$. The decrease of κ with the increase of Li concentration certainly is due to the enhanced scattering of phonons by the substitution of Li for Ni.

The relationship between electrical conductivity σ and temperature is presented in Fig. 5. We observed that σ of all samples monotonously increases with the increase of temperature, showing a behavior of semiconductor. Moreover, we can also find that σ increases with the increase of Li concentration. Compared to other samples, $Ni_{0.91}Li_{0.09}O$ shows a higher σ value in the whole measuring temperature range. This increase of σ should owe to L doping, because Li doping increases the hole carrier concentration and Li is a effective source for hole carrier generation [12]. And according to the expression $\sigma = pe\mu$ (where p is the carrier concentration, e is the electron charge and μ is the carrier mobility), the increase of σ with Li doping amount is due to the increase of the hole concentration.

The activation energy of conduction (E_a) of the $Ni_xLi_{1-x}O$ was calculated through the equation $\sigma = \sigma_0 \exp(E_a/k_BT)$, where k_B is the Boltzmann constant. The literature reported E_a is 0.528 eV for pure NiO. From Table 1, it can be seen that E_a decrease with the increase of Li doping amount, which means that more carriers are produced by Li doping and therefore σ is enhanced accordingly.

The temperature dependence of Seebeck coefficient α for $Ni_{1-x}Li_xO$ samples is shown in Fig. 6. The α of all samples are positive in the entire temperature range, indicating a p-type semiconductor behavior and α decrease with the increase of temperature for all samples. In addition, with the increase of Li

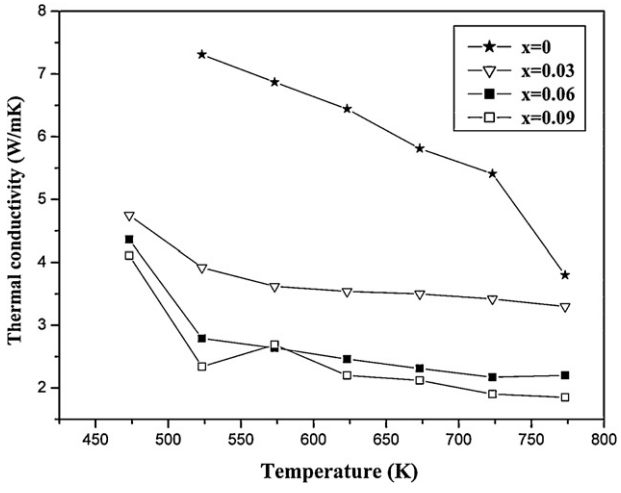

Fig. 4. Temperature dependence of thermal conductivity for $Ni_{1-x}Li_xO$ samples.

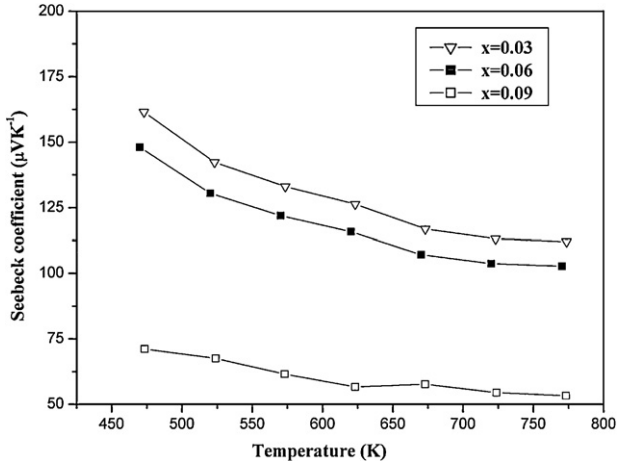

Fig. 6. Temperature dependence of Seebeck coefficient for $Ni_{1-x}Li_xO$.

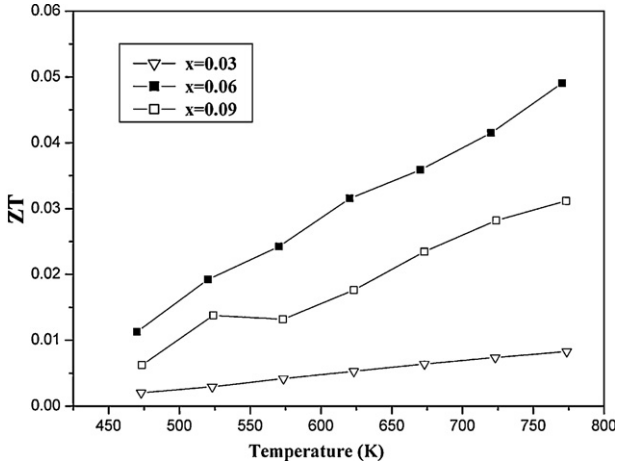

Fig. 7. Temperature dependence of the figure of merit for $Ni_{1-x}Li_xO$.

concentration, the value of α has an obvious reduction. The maximum α values of $Ni_{0.97}Li_{0.03}O$ is 161 μV/K at 473 K, while that of $Ni_{0.91}Li_{0.09}O$ is only 71 μV/K. These results imply that the substitution of Li for Ni in the NiO will result in a decrease of the Seebeck coefficient.

The thermoelectric figure of merit (ZT) of the $Ni_xLi_{1-x}O$ were calculated from the data above, according to $ZT = \alpha^2\sigma T/\kappa$. As shown in Fig. 7, the highest value of ZT is 0.049 at 770 K for the 6% Li-doped sample, and the increase trend with temperature increase suggests that the value of ZT will be much higher if temperature is further increased.

4. Conclusions

$Ni_{1-x}Li_xO$ ($x = 0$, 0.03, 0.06, 0.09) samples have been successfully prepared by sol–gel method combined with sintering procedure. The XRD patters indicated that there are no impure phases existence when replace Ni by Li. The Li doped samples are p-type semiconductors. The electrical conductivity increases with the increase of the temperature. On the one hand, substitution of Li^+ for Ni^{2+} increases the concentration and mobility of the carriers, which results in an increase of the electrical conductivity, however, it also cause a decrease of the Seebeck coefficient inevitably. On the other hand, substitution of Li^+ for Ni^{2+} can enhance the scattering of phonons, which brings a remarkable decrease of the thermal conductivity. As results of the increase of the electrical conductivity and the reduction of the thermal conductivity, Li doping can increase the ZT value of NiO.

References

[1] H.C. Wang, C.L. Wang, W.B. Su, J. Liu, H. Peng, Y. Sun, J.L. Zhang, M.L. Zhao, J.C. Li, N. Yin, L.M. Mei, Synthesis and thermoelectric performance of Ta doped $Sr_{0.9}La_{0.1}TiO_3$ ceramics, Ceram. Int. 37 (2011) 2609–2613.
[2] Y.F. Wang, K.H. Lee, H. Ohta, K. Koumoto, Fabrication and thermoelectric properties of heavily rare-earth metal-doped $SrO(SrTiO_3)_n$ (n = 1, 2) ceramics, Ceram. Int. 34 (2008) 849–852.
[3] F. Li, J.F. Li, Effect of Ni substitution on electrical and thermoelectric properties of $LaCoO_3$ ceramics, Ceram. Int. 37 (2011) 105–110.
[4] W. Luan, Y.J. Shan, M. Itoh, H. Imoto, Preparation and thermoelectric properties of $Cd_{3-x}A_xTeO_6$ (A = In, La, and Bi) ceramics, Ceram. Int. 31 (2005) 129–133.
[5] D.H. Kim, C. Kim, D.W. Ha, H. Kim, Fabrication and thermoelectric properties of crystal-aligned nano-structured Bi_2Te_3, J. Alloys Compd. 509 (2011) 5211–5215.
[6] D.Q. Lu, G. Chen, J. Pei, X. Yang, H.Z. Xian, Effect of erbium substitution on thermoelectric properties of complex oxide $Ca_3Co_2O_6$ at high temperatures, J. Rare Earth 26 (2008) 168–172.
[7] W. Shin, N. Murayama, K. Ikeda, S. Sago, Thermoelectric power generation using Li-doped NiO and $(Ba,Sr)PbO_3$ module, J. Power Sources 103 (2001) 80–85.
[8] J.F. Wang, J.N. Cai, Y.H. Lin, C.W. Nan, Room-temperature ferromagnetism observed in Fe-doped NiO, Appl. Phys. Lett. 87 (2005) 202501.
[9] R.H. Kodama, S.A. Makhlouf, A.E. Berkowitz, Finite size effects in antiferromagnetic NiO nanoparticles, Phys. Rev. Lett. 79 (1997) 1393–1396.
[10] S. Manna, A.K. Deb, J. Jagannath, S.K. De, Synthesis and room temperature ferromagnetism in Fe doped NiO nanorods, J. Phys. Chem. C 112 (2008) 10659–10662.
[11] H.X. Yang, Y.G. Shi, X. Liu, R.J. Xiao, H.F. Tian, J.Q. Li, Structural properties and cation ordering in layered hexagonal Ca_xCoO_2, Phys. Rev. B 73 (2006) 014109.
[12] W. Shin, N. Murayama, High performance p-type thermoelectric oxide based on NiO, Mater. Lett. 45 (2000) 302–306.